Climate forcing reconstructions for use in PMIP simulations of the last millennium (v1.0)

G.A. Schmidt, J.H. Jungclaus, C. M. Ammann, E. Bard, P. Braconnot, T. J. Crowley, G. Delaygue, F. Joos, N. A. Krivova, R. Muscheler, et al.

Geosci. Model Dev., 4, 33–45, 2011
www.geosci-model-dev.net/4/33/2011/
doi:10.5194/gmd-4-33-2011

Geoscientific Model Development

Climate forcing reconstructions for use in PMIP simulations of the last millennium (v1.0)

G. A. Schmidt[1], J. H. Jungclaus[2], C. M. Ammann[3], E. Bard[4], P. Braconnot[5], T. J. Crowley[6], G. Delaygue[7], F. Joos[8,15], N. A. Krivova[9], R. Muscheler[10], B. L. Otto-Bliesner[3], J. Pongratz[11], D. T. Shindell[1], S. K. Solanki[9,12], F. Steinhilber[13], and L. E. A. Vieira[14]

[1]NASA Goddard Institute for Space Studies and Center for Climate Systems Research, Columbia University, New York, USA
[2]Max-Planck-Institute for Meteorology, Bundesstrasse 53, 20146 Hamburg, Germany
[3]National Center for Atmospheric Research, 1850 Table Mesa Drive, Boulder, Colorado, USA
[4]CEREGE, Université Aix-Marseille III/CNRS/IRD/Collège de France, Europôle de l'Arbois, BP 80, 13545 Aix-en-Provence Cedex 04, France
[5]Laboratoire des Sciences du Climat et de l'Environnement, Gif Sur Yvette, France
[6]School of GeoSciences, University of Edinburgh, Edinburgh, UK
[7]Université Joseph Fourier-Grenoble I/CNRS, LGGE, 54 rue Molière, St-Martin-d'Hères, France
[8]Climate and Environmental Physics, Physics Institute, University of Bern, Sidlerstrasse 5, 3012 Bern, Switzerland
[9]Max-Planck-Institut für Sonnensystemforschung, 37191 Katlenburg-Lindau, Germany
[10]Department of Earth and Ecosystem Sciences, Lund University, Sölvegatan 12, 22362 Lund, Sweden
[11]Carnegie Institution of Washington, Department of Global Ecology, 260 Panama St., Stanford, CA 94305, USA
[12]School of Space Research, Kyung Hee University, Yongin, Gyeonggi 446-701, Korea
[13]Swiss Federal Institute of Aquatic Science and Technology, EAWAG, Überlandstrasse 133, 8600 Dübendorf, Switzerland
[14]Laboratoire de Physique et Chimie de l'Environnement et de l'Espace and Université d'Orléans, 3A, Avenue de la Recherche, 45071 Orléans cedex 2, France
[15]Oeschger Centre for Climate Change Research, University of Bern, 3012 Bern, Switzerland

Received: 21 August 2010 – Published in Geosci. Model Dev. Discuss.: 27 September 2010
Revised: 2 December 2010 – Accepted: 21 December 2010 – Published: 21 January 2011

Abstract. Simulations of climate over the Last Millennium (850–1850 CE) have been incorporated into the third phase of the Paleoclimate Modelling Intercomparison Project (PMIP3). The drivers of climate over this period are chiefly orbital, solar, volcanic, changes in land use/land cover and some variation in greenhouse gas levels. While some of these effects can be easily defined, the reconstructions of solar, volcanic and land use-related forcing are more uncertain. We describe here the approach taken in defining the scenarios used in PMIP3, document the forcing reconstructions and discuss likely implications.

Correspondence to: G. A. Schmidt
(gschmidt@giss.nasa.gov)

1 Introduction

As part of the lead up to the Intergovernmental Panel on Climate Change (IPCC) Fifth Assessment report (AR5), modelling groups around the world are coordinating a series of simulations under the umbrella of the fifth Coupled Model Intercomparison Project (CMIP5, http://cmip-pcmdi.llnl.gov/cmip5/, Taylor et al., 2009). These simulations will cover the 20th century, various scenarios into the future and three paleo-climate simulations for the Last Glacial Maximum (LGM), the mid-Holocene (MH) and the Last Millennium (LM) in collaboration with the existing Paleoclimate Model Intercomparison Project Phase III (PMIP3 http://pmip3.lsce.ipsl.fr/, Otto-Bliesner et al., 2009). This paper will discuss the choices made in determining the climate forcings for the LM simulations.

Published by Copernicus Publications on behalf of the European Geosciences Union.

The LM simulations will start in 850 Common Era (CE) and go to 1850 CE where they are expected to match up and continue with the 1850–2005 simulations that are also being prescribed by CMIP5. The start date is determined by the lack of availability of some forcings prior to that period, and a desire to have the transient simulation start earlier than the classic Medieval period (1000–1200 CE). While the precise timing of the "Medieval Warm Period" or (preferably) the "Medieval Climate Anomaly" varies widely in the literature, there is strong interest in the most recent period whose mean temperature anomalies may have been comparable to the present-day (e.g., Bradley et al., 2003; Osborn and Briffa, 2006; Mann et al., 2009). A start at 850 CE ensures that the models will be able to cover all the relevant periods.

It is likely that these experiments will be used to quantify the response of the models to forcings in the past in order to weight projections into the future (Schmidt, 2010), and in detection and attribution studies (Hegerl et al., 2007). The experiments described below are thus intended to be as realistic a description of past forcings and response as possible, while trying hard to ensure that the uncertainties in the forcings are properly represented. This has lead us to suggest a number of alternate forcing histories for volcanic and solar changes rather than specifying that all models use a single, arbitrarily chosen, one. This approach is different from the one adopted for previous PMIP experiments, which requested that all modeling groups used similar forcing in order to favor model intercomparisons (Joussaume and Taylor, 1995; Braconnot et al., 2007).

The novel aspect in CMIP5 of having the same models and configurations used in the paleo-climate simulations as with the transient 20th century and future simulations implies that consistency – both in the overall forcings and in how they are imposed – with those other experiments is a very strong requirement. This constraint has motivated most of the choices described below and is one of the main differences between these experiments and previously reported simulations of this period (Jansen et al., 2007, Table 6.2).

This has a number of implications: For instance, in order not to bias simulations of decadal variability, solar reconstructions need to have a consistent representation of the quasi-11-year cycle through the record. This requires a synthetic cycle to be applied prior to 1610. Similarly, if spectral variations in solar irradiance are included in the 20th century transient runs, then these variations need to be maintained over the whole period. Furthermore, many of the 20th century simulations will be run with interactive chemistry. This will allow for variations in stratospheric and tropospheric ozone as a function of the incoming solar UV, which varies both in the long term and over a solar cycle.

Since some aspects of these reconstructions are unconstrained (more so in the earlier periods), the procedure we adopt here is admittedly ad-hoc, though plausible. Other choices could be made, but these will not greatly affect the range of forcings through time. Our aim is not to produce definitive reconstructions, but to allow the structural uncertainty in these reconstructions to be tested in a coherent environment.

2 Forcings over the last millennium

We describe here the first-order forcing functions that are relevant for this period (Table 1). This choice is determined by the availability of data and our current state of knowledge, and is therefore not anticipated to be a complete accounting. Other forcings, for instance related to dust or other aerosols, may have played a role, but cannot at this time be specified sufficiently for use in an intercomparison such as this. All timeseries and reconstructions are available via the Supplement and online at the PMIP3 website.

2.1 Orbital variations

Over the period 850 CE to present, the principal orbital change is the $\sim$20 day shift in the perihelion from 15 December to 4 January, leading to a progressive increase in insolation in the early Northern Hemisphere summer relative to the later part (Berger, 1978; Laskar et al., 2004). There are also small decreases in eccentricity and obliquity. These shifts cause a decrease of about $9\,\mathrm{W m^{-2}}$ in August, and an increase of $3\,\mathrm{W m^{-2}}$ in May, in high northern latitudes. In the Southern Hemisphere, there is a decrease of a few watts in November, and a similar increase in February (Fig. 1).

2.2 Well-mixed greenhouse gases

Variations in the principal well-mixed greenhouse gases (CO_2, CH_4 and N_2O) can be derived from high resolution ice cores in Antarctica. Law Dome results are used exclusively for CO_2 and CH_4 (Etheridge et al., 1996, 1998; Ferretti et al., 2005; MacFarling Meure et al., 2006), while for N_2O multiple cores are used in order to get a more robust signal (Flückiger et al., 1999, 2002; Machida et al., 1995). These variations have been tied to the post-1850 record (Hansen and Sato, 2004) using a spline fit, after adjusting the CH_4 record for the difference between the global mean and Antarctic values (16 ppb for CH_4), and smoothing so that only decadal-scale and longer variations are retained (Joos and Spahni, 2008); a nominal cut-off period of 40 years was applied for CO_2 and CH_4 and of 100 years (200 years before 1600 CE) for N_2O (Fig. 2).

The variations seen are related both to natural feedbacks in the carbon and nitrogen cycles to changes in climate, but also some initial anthropogenically drive perturbations, although the attribution of these relatively small changes prior to the industrial period is difficult (Gerber et al., 2003).

Table 1. Summary of Last Millennium boundary conditions.

Feature	PMIP3 recommendation	Alternate solution
Orbital parameters	Annually varying	
Date of vernal equinox	21 March at Noon	
Well-mixed greenhouse gases	Annually varying	
Volcanic aerosols	Two reconstructions (AOD, effective radius): GRA (Gao et al., 2008) CEA (Crowley et al., 2008)	
Solar irradiance	Multiple reconstructions (including spectral variations): WLS (back/noback)* (Wang et al., 2005) 1610–2005 VSK (Vieira et al., 2010) 850–1850 and merge to WLS (back) SBF (Steinhilber et al., 2009) 850–1850 and merge to WLS (back) MEA (back/noback) (Muscheler et al., 2007) 850–1610 and merge to WLS (back/noback) DB (back/noback) (Delaygue and Bard, 2010) 850–1610 and merge to WLS (back/noback)	
Ozone	Parameterisation of solar-related variations	Same as PI-control**
Tropospheric aerosols	Not prescribed	Same as PI-control
Vegetation	Land cover change (natural vegetation to crop/pasture)	Same as PI-control
Ice sheets	No changes from PI-control	
Topography and coastlines	Same as in PI-control	

* The terms "back/noback" denote a solar reconstruction that does/does not include a background variation in irradiance above that driven by the 11 year cycle alone.
** PI-control is the pre-industrial CMIP5 control simulation (conditions circa 1850).

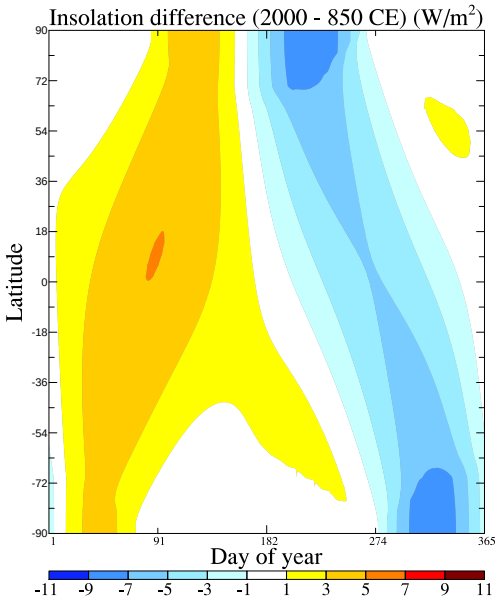

Fig. 1. Insolation difference (2000–850 CE) (Wm^{-2}) as a function of latitude and Julian day.

2.3 Land use/land cover (LULC)

The reconstruction of LULC adopted by PMIP (Pongratz et al., 2008) covers the time period 800 to present day. It is based on published maps of agricultural areas for the last three centuries and a country-based approach for earlier times that uses population data as a proxy for agricultural activity. The resulting dataset contains annual maps of the agricultural types cropland, C3 pasture, and C4 pasture (Fig. 3). Allocation rules were developed that determine which type of natural vegetation within a grid cell is affected by the reconstructed changes in agriculture, and extend the dataset to include area changes of natural vegetation (eleven types of forest, shrubland, and grassland). This land cover change has a direct impact on the albedo of the surface, but also indirect impacts on water cycling, surface roughness and soil characteristics. There is also an implied impact for CO_2 emissions and CO_2 uptake capacity of the terrestrial biosphere, but which are not considered here since they are implicit in the greenhouse gas concentration changes described above.

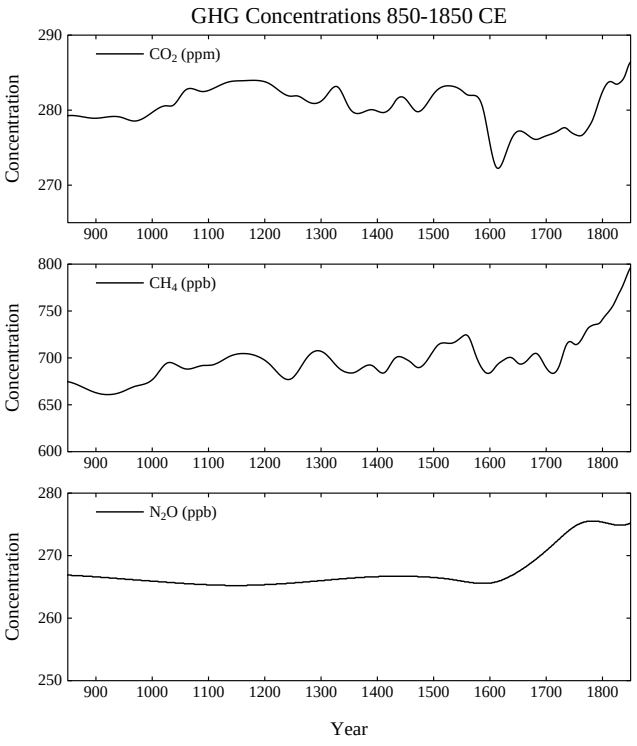

Fig. 2. Well-mixed greenhouse gas concentration changes from 850 to 1850 CE.

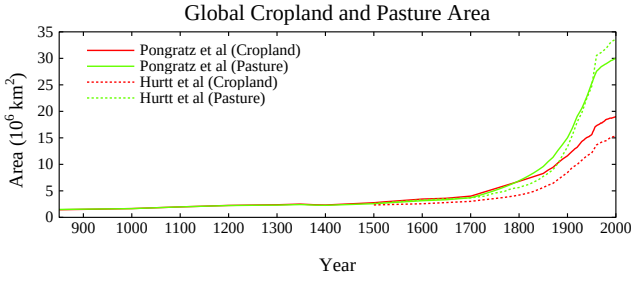

Fig. 3. Global mean cropland and pasture area in the Pongratz and Hurtt datasets.

The reconstruction can be used through to the present day, with the more recent (1700 onwards) land use changes equivalent to those in the Ramankutty and Foley (1999) dataset with some regional modifications. However, for the simulations of the future scenarios for AR5, many modeling groups have adopted a recent synthesis of LULC data (Hurtt et al., 2009). This dataset was developed to harmonize historical LULC data, based on HYDE3.0 (Klein Goldewijk and van Drecht, 2006) from 1500 to present, with the various future scenarios of the Integrated Assessment Models. It indicates gridded area and transitions between a limited number of land use classes (cropland, pasture, urban area, primary vegetation, and secondary vegetation). The type of primary or secondary vegetation (forest, grassland, etc.) has to be determined by each climate model, e.g. from their dynamic vegetation modules or from maps of potential vegetation. Unlike for the Pongratz et al. (2008) dataset, no allocation rules are provided. "Secondary vegetation" is natural vegetation that at some point in the past has been affected by land use. This land use includes shifting cultivation and wood harvesting effects, neither of which is explicitly included in the Pongratz et al. (2008) dataset. Due to the lack of suitable input information, Hurtt et al. (2009) assume zero secondary vegetation in the year 1500.

For a continuous time series of LULC data from 800 to the future scenarios melding the two datasets may be necessary for some modelling groups depending on the configuration and capabilities of their land model. There are natural discontinuities at 1500, 1700 and 1850 CE resulting from switches in input data sources, which might serve as good splice points. At the merge point, the changes in cropland and pasture area from the Pongratz et al. (2008) dataset can be scaled or applied on a grid cell-by-grid cell basis, unless area changes exceed the grid cell's available agricultural or land area. The surplus changes in cropland and pasture could then be distributed on other grid cells within the same country. Due to the lack of wood harvest data prior to 1700, we suggest setting the ratio of secondary vegetation to agricultural area constant at the merge point value for prior years.

Uncertainties in the Pongratz et al. (2008) reconstruction can be assessed by using the maximum and minimum alternate reconstructions also available.

2.4 Volcanic forcing of stratospheric aerosols

Gao et al. (2008) (hereafter GRA) and Crowley et al. (2008) (hereafter CEA) provide two different reconstructions of aerosol optical depth due to volcanoes from stacks of well-dated ice core sulphate records from both polar regions. They differ in the transfer function for the sulphate ice core concentrations to aerosol optical depth (AOD) and in the screening processes for deciding what is and is not a globally important eruption. Cores from both Greenland and Antarctica are used to determine whether any particular peak is local, hemispheric or global in extent and thus likely to have reached the stratosphere. Historical records of eruptions are used to assign peaks to specific years and assess the likely extent of the resulting sulphates.

2.4.1 Implementation

The GRA procedure is to estimate the total stratospheric aerosol load and then use a model based estimate of the latitudinal, height and time distribution of the aerosols. The provided files contain estimates of the stratospheric aerosol loadings (kg SO_4 km^{-2}) which can be converted into a global AOD by linear scaling (Stothers, 1984). The conversion to AOD is valid for aerosols with effective radius in the visible

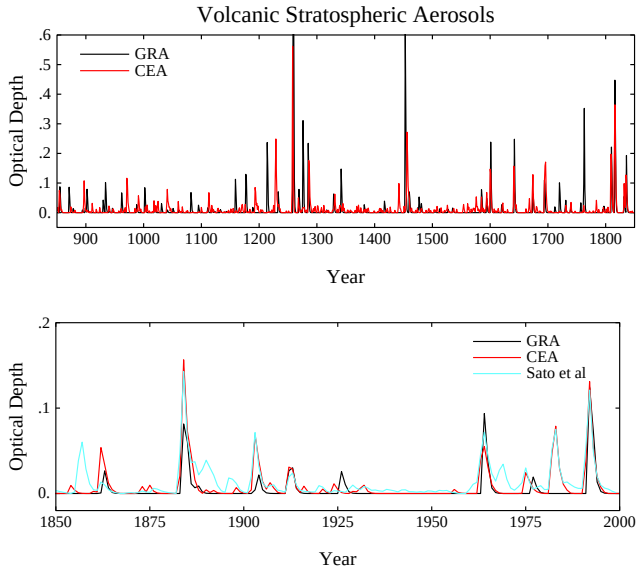

Fig. 4. The two volcanic reconstructions of aerosol optical depth (at 550 µm) (GRA and CEA) (top), with a comparison to the modern estimates of Sato et al. (1993) (bottom) (note the different vertical scales in the two panels).

spectral range. CEA provide an estimate of AOD directly from a scaling with modern observational estimates and from the evolution of the Pinatubo aerosols. The load can be estimated by reversing the above scaling.

The difference in the two reconstructions can be seen in Fig. 4 (including the 20th century to allow comparison with the Sato et al., 1993 data). Different events are captured in each case, and different amplitudes are often inferred.

In the modern period, the dataset of Sato et al. (1993) (and updates) also includes variations in the effective radius (r_e in µm) of the aerosol particles based on observations of changes from El Chichon (1982) and Pinatubo (1991):

$$r_e = 0.20 + \tau_{max}(\phi) \times 0.75 \times f(t - t_0)$$

where $\tau_{max}(\phi)$ is the maximum optical depth at each latitude for each eruption and $f(t)$ is a decay function (peaking at 1.3 years and decaying to zero at 5 years). The details of this process may be relevant to the apparent non-linear response to large volcanoes in the past (Timmreck et al., 2009), and is another source of uncertainty in these reconstructions.

CEA include estimates of aerosol size, scaling to Pinatubo r_e for eruptions up to that magnitude and for eruptions greater than 0.2 AOD, they use a two-thirds power scaling for AOD and a one-third power scaling of the AOD for r_e, with maximum estimate of r_e about 0.9 µm. For the GRA reconstruction, either recipe (or none) for r_e may be used.

2.5 Solar variations

Changes in irradiance are the most important known component of solar activity that affects climate. Other aspects of solar activity – for instance, the role of sun's magnetic field in shielding the planet from cosmic ray particles and possibly affecting clouds (Ney, 1959; Dickinson, 1975) are generally correlated to irradiance changes at least over decadal periods.

Observations over the 30-year satellite period confirm that there is a quasi-11 yr cycle in total solar irradiance (TSI) in phase with sunspot activity, and that the spectral signature of the irradiance variations is distinct, with higher energy frequencies (UV, X-ray etc.) varying more strongly over the cycle than the TSI (Lean et al., 1995; Floyd et al., 2003; Harder et al., 2009). Models for the irradiance have been successful at matching the observations based on sunspot numbers, magnetic activity and the area of bright faculae surrounding the sunspots (Fröhlich and Lean, 1998; Krivova et al., 2003; Wenzler et al., 2006). However, there is some debate over whether there is a background variation in irradiance (the "network") that is not easily determinable from observations of current activity (Foukal et al., 2006; Wang et al., 2005; Krivova et al., 2007), although the lower irradiance level during the minimum following solar cycle 23 (i.e. in the years 2007–2009) suggests that there is indeed such a variation.

Prior to the satellite era, solar activity can be tracked by various proxy instrumental and geophysical measurements. Over longer time periods, there are records of cosmogenic isotopes such as ^{14}C in tree-rings, and ^{10}Be or ^{36}Cl in polar ice cores. These are formed by the nuclear reactions between cosmic ray particles and atoms in the atmosphere and increase in abundance in anti-phase with solar activity. Connecting these proxies to the short record of satellite-derived solar irradiance is however difficult both technically and theoretically. For instance, many of the proxies do not overlap with the modern instruments: ^{14}C records have been contaminated by anthropogenic fossil carbon releases and atmospheric nuclear bomb tests, some ^{10}Be records do not have very good resolution in the 20th century and varying trends, and there have been measurement practice changes through time in sunspot counts, geomagnetic indices and cosmic ray intensity. The theoretical difficulties are also important. First, there is a small impact of historical geomagnetism changes on cosmic ray shielding. Second, the factors that affect open solar magnetic field are uncertainly linked to solar irradiance, though much work is being done to elucidate the connection (Wang et al., 2005; Krivova et al., 2007; Vieira et al., 2010). Additionally, the relationships of the cosmogenic archives to global mean production levels may be themselves somewhat affected by climate (Field et al., 2009; Heikkilä et al., 2008). Nonetheless, there is sufficient qualitative overlap of the different proxies where they are available to combine them quantitatively to produce a homogeneous record of solar activity back through time (Vonmoos et al., 2006; Usoskin et al., 2009).

2.5.1 Available input data

The raw material out of which the solar reconstructions are built consists of: (i) direct satellite observations of TSI since 1978 (Fröhlich, 2009), (ii) the Mg II index (from 1978) (Viereck et al., 2004), (iii) Magnetograms (from 1974) (Wenzler et al., 2004), (iv) F10.7 radio flux (from 1947) (Tanaka et al., 1973), (v) instrumental records of cosmic ray intensity from neutron monitor counting rates since 1951 and ionization chambers back to 1933 (McCracken and Heikkila, 2003; McCracken and Beer, 2007), (vi) geomagnetic indices like the aa-index (from 1868) or IHV index (from 1901) (Lockwood et al., 1999; Clilverd et al., 2005; Svalgaard et al., 2004; Rouillard et al., 2007), (vii) group sunspot numbers (from 1610) (Hoyt and Schatten, 1998), (vii) Cosmogenic isotope production rates from ^{14}C concentrations (Muscheler et al., 2007; Reimer et al., 2009) (up to ∼1950), and from multi-centennial ^{10}Be records from Greenland (Yiou et al., 1997; Beer et al., 1998; Muscheler et al., 2004; Berggren et al., 2009) and Antarctica (Raisbeck et al., 1990; Horiuchi et al., 2008). Each data source has its own issues with resolution, age control, measurement uncertainty, confounding factors and interpretation, and calibrating them all to the same modern measurements is complicated.

First, the satellite measurements need to be combined into a consistent timeseries (Fröhlich and Lean, 1998; Willson and Mordvinov, 2003; Dewitte et al., 2004). Unfortunately, there is a gap between good satellite measurements from mid-1989 to fall 1991 which has complicated this procedure. Three composite records have been published that vary slightly in value of the solar minimum around 1996 and 2009, though recent studies support the use of the Physikalisch-Meteorologisches Observatorium Davos (PMOD) composite (Krivova et al., 2009; Gray et al., 2010). Then a model (either statistical or physically-based) must be constructed for the relationship between the irradiance and other aspects of solar activity (Lean et al., 1995; Balmaceda et al., 2007; Fröhlich, 2006). Using the available instrumental data and these models, the reconstructions can be taken back at least to the 19th century. Reconstructions back to 1610 are possible using the sunspot data using various assumption about how sunspots relate to the facular and network evolution.

Wang et al. (2005) (hereafter WLS) use a physically-based model for the "open flux" and have produced two reconstructions back to 1610, one with and one without an independent change in the background level of irradiance (the "no-background" case). Alternately, Balmaceda et al. (2007) and Krivova et al. (2007) use a physically-based model of the evolution of the total solar surface magnetic field. Note that the WLS reconstructions (along with the spectral variations, Lean, 2009) are the recommended solar forcings for the CMIP5 20th century (1850 onwards) simulations.

Before 1610, reconstructions must rely on the cosmogenic isotopes, principally ^{10}Be and ^{14}C. Taking past variations of the geomagnetic field into account, the solar activity (described by the solar modulation function Φ) can be obtained from the isotope records. However, the relationship between Φ and irradiance is complicated (Usoskin et al., 2002; Steinhilber et al., 2009). At least four groups have proposed Φ reconstructions from cosmogenic isotopes. Two of them (Muscheler et al., 2007; Delaygue and Bard, 2010) (hereafter MEA and DB) did not make an independent physical calibration to irradiance, and so we use a linear relation derived from the WLS modern-to-Maunder Minimum differences. Two other groups have used a chain of physically-based models to link Φ to irradiance using either the observed long-term relationship between total solar irradiance and open solar magnetic field (Fröhlich, 2009; Steinhilber et al., 2009, hereafter SBF) or a physical modeling of the solar surface magnetic flux and its relationship with the isotopes (Vieira et al., 2010, hereafter VSK).

2.5.2 Solar reconstructions for PMIP

As discussed above, each reconstruction for use in a GCM needs to have: TSI values back to 850, a solar cycle (of varying amplitude) over the whole record and spectral variations consistent with those changes.

We calibrate all the TSI variations to have the same value in the modern period. We choose to use the 1976–2006 mean (approximately 3 cycles) from the WLS reconstruction (1366.14 $\mathrm{W m^{-2}}$). Recent estimates from the SORCE/TIM instrument suggest that the absolute value for the mean solar irradiance is closer to 1361 $\mathrm{W m^{-2}}$ (Kopp et al., 2005), but for any models that use this or a different modern TSI (e.g., Mekaoui et al., 2010), we suggest simply scaling everything by a suitable factor.

We define a long-term mean TSI using a 40 year triangular filter. A standard "11-year" cycle is found by taking the maxima in the 20th century record of WLS no-background case, calculating the anomaly from the 40 yr smooth, normalising the cycle by the maximum value and averaging over the cycles to give a fixed 11-year shape (Fig. 5).

Since the maximum of a solar cycle is correlated to the 40 year smooth TSI anomaly (Fig. 6), we can use this relationship to define a scaling between the long-term smoothed reconstruction anomaly and a plausible solar cycle:

$$\mathrm{SC_{max}} = \max\left(0, \bar{S}(t_{\max}) + 0.433\left(\bar{S}(t_{\max}) - \bar{S}(t_{\mathrm{MM}})\right)/\Delta S\right)$$

where $\mathrm{SC_{max}}$ is the solar cycle maximum anomaly at time $t_{\max}$, $\bar{S}(t)$ is the smoothed TSI time-series, $\bar{S}(t_{\mathrm{MM}})$ is the value of the irradiance at the Maunder Minimum (MM) in any specific reconstruction, and ΔS is the difference in smoothed TSI between the MM and modern. For values of TSI at or below MM values, we set the solar cycle magnitude to zero. Using an alternate scaling as illustrated in Fig. 6 would increase the amplitude of the cycles by about 20%.

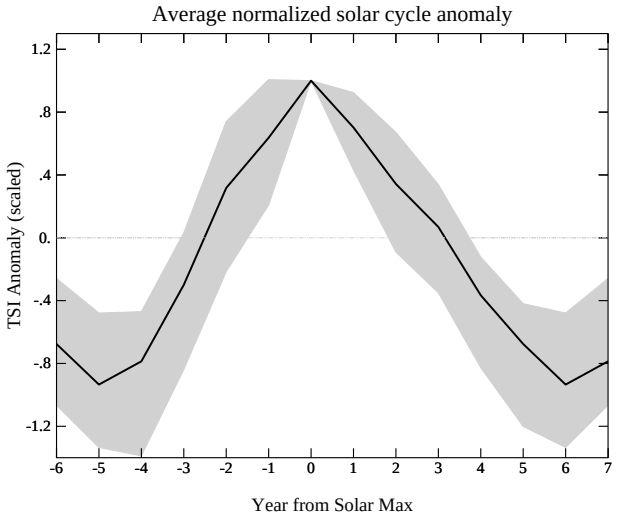

Fig. 5. Normalised mean solar cycle anomaly with respect to the 40-year smoothed irradiance, derived from the no-background data of WLS. Greyscale is one standard deviation from the underlying individual cycles.

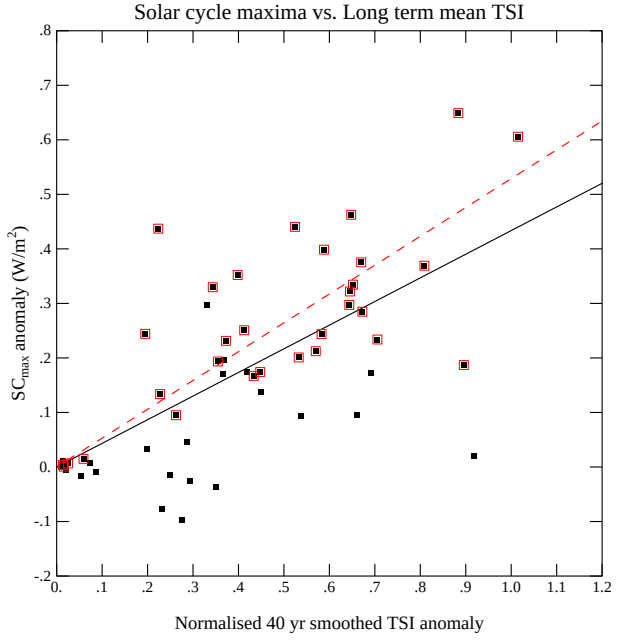

Fig. 6. Solar cycle maxima versus the 40-year smoothed irradiance data from WLS. Linear regression through the origin using all local maxima (solid line) gives SC_{max}=0.433 $(\bar{S}(t_{max})-\bar{S}(t_{MM}))/\Delta S$, ($r^2$=0.47). Note that a tighter screening of which points count as solar cycle maxima and only using local maxima that exceed the long-term mean (overlain red symbols) gives a slightly steeper regression of 0.53, (r^2=0.56) (dashed line).

Spectral solar irradiance (SSI) variations occur over solar cycles and the longer term, but are not purely related to the TSI value because of the different influences of sunspots

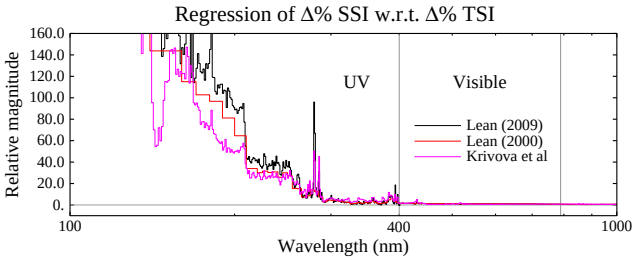

Fig. 7. Spectral variations of irradiance relative to the variation in TSI (regression of the % change in SSI at each wavelength to the % change in TSI). A relative magnitude of 20 implies that variations at that wavelength would be around 2% over a cycle, i.e. 20× the ∼0.1% variation in TSI. The reference period used for the Lean (2009) and Krivova et al. (2010) curves are from the Maunder Minimum (1645–1715), while it is 1850 for Lean (2000). Note there are fewer wavelength bands in the older data.

and faculae on different time scales at different wavelengths (Lean, 2000). However, linear regressions of TSI with the irradiance at each spectral interval explain around 97% of the variance at most wavelengths, implying that TSI can be used as a reasonable first-order predictor of the SSI prior to 1610. The regression of the WLS with-background TSI with the Lean (2009) SSI shows that the UV portions of the spectra have a much higher percentage variation over solar cycles (and presumably, longer time scales) than TSI (Fig. 7). Note that a number of different estimates of the spectral variations are emerging from new data and models (Krivova et al., 2010; Harder et al., 2009) but are not yet available for these purposes.

For the two long term reconstructions of Φ, we calibrate them directly to the WLS reconstructions back to 1610 (and for both the background and no-background cases) and produce a consistent reconstruction from 850 to 1609 which smoothly blends into the WLS values and the solar cycle phase. For the two reconstructions (VSK and SBF) that have independent calibrations to the Maunder Minimum values (one slightly greater in amplitude than the WLS with background case, one slightly smaller), we smoothly join the reconstructions in 1850 to the WLS with background values. We choose 1850 in these cases since the structure of the modern cycles is more accurate in the WLS values, and so that there is maximum coherence with 20th century transients. Other splice years are possible and could be examined in additional sensitivity experiments.

Thus, we present a series of six alternative reconstructions (Fig. 8) that differ in their source data, processing, and calibration. Two of the six match up to the no-background WLS case, two match up with the WLS with-background case, and two others provide alternate estimates of the changes at the Maunder Minimum (matching up to WLS with-background in 1850). If a modelling group is using

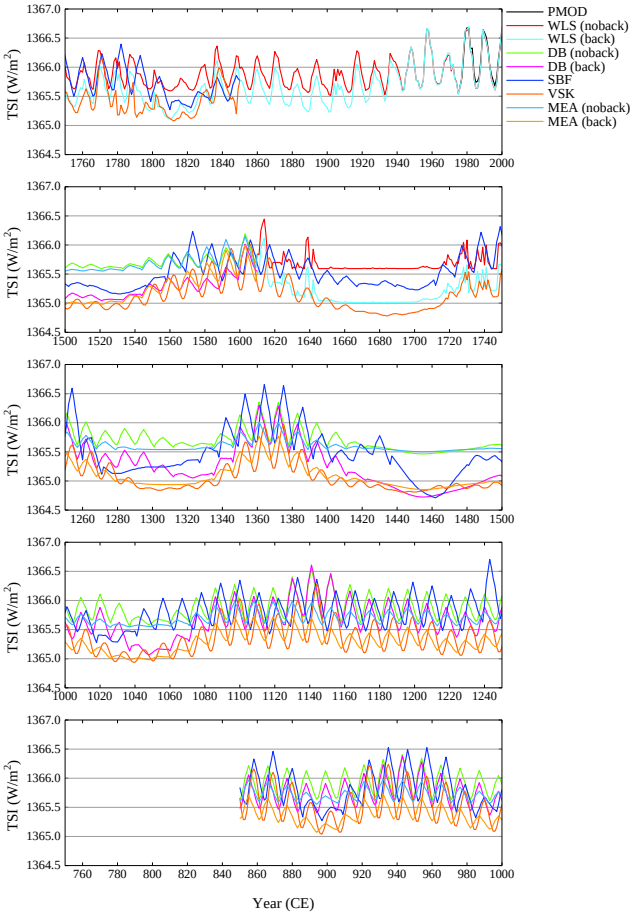

Fig. 8. Multiple TSI reconstructions from 850 CE onwards, with the PMOD satellite-based TSI composite as reference.

the WLS no-background case for the 20th century, they have a choice of two alternative continuations back to 850, while if they use the with-background case, they have a choice of four independent reconstructions for the earlier period. There are also four alternate estimates of TSI during the Maunder Minimum (and any earlier grand minima).

The decrease in TSI at the Maunder Minimum (defined here as the 40-year smoothed value at 1680) compared to the modern average is a 0.04% decrease for the WLS no-background reconstructions, 0.08% for WLS with-background, 0.06% for SBF, and 0.10% for VSK. The corresponding radiative forcings are between 0.10 and 0.23 $\mathrm{W m^{-2}}$ and are close to the best estimate given by IPCC AR4 (Forster et al., 2007, Table 2.10) of 0.19 $\mathrm{W m^{-2}}$. These changes are substantially smaller than seen in some earlier reconstructions (e.g., Hoyt and Schatten, 1998). However, the calibrations for the Maunder Minimum used previously are no longer justifiable in the light of new information and so are not considered here (Foukal et al., 2006; Forster et al., 2007; Gray et al., 2010).

2.5.3 Solar-related ozone changes

In order to better match up with 20th century simulations that include interactive chemistry and specifically allow ozone to vary as a function of incoming UV, we have made available a parameterisation of the solar-derived ozone changes taken from a coupled chemistry-climate model (Shindell et al., 2006). This can be used in non-interactive runs as a modification of the basic ozone fields that is in phase with the solar activity and scales with the strength of the total solar irradiance variation relative to the modern mean value.

The ozone fields come from model calculations performed for modern-day solar maximum and minimum conditions. This corresponds to a 1.1 $\mathrm{W m^{-2}}$ irradiance change at the top of the atmosphere and includes spectral variations from Lean (2000) (Fig. 7), with the difference between equilibrium responses averaged over 70 years of model output. Ozone in the middle stratosphere increases with irradiance, with a maximum enhancement of ∼2.5% at 10 hPa. Increases are largest in the tropics and mid-latitudes. The magnitude of change decreases above and below the middle stratosphere, becoming negative above ∼1 hPa. These results are similar to those seen in other photochemical models. Modern satellite observations are consistent in showing increases in stratospheric ozone with irradiance of 0–3%, but differ in both the vertical and latitudinal dependence of the increases (e.g., Soukharev and Hood, 2006).

In the original modelling study (Shindell et al., 2006), these ozone changes increased stratospheric temperatures mostly around 1 hPa, with a maximum of ∼0.6–0.7 °C at mid-latitudes in both hemispheres. Warming extended throughout the atmospheric column, though values were small in the troposphere (<0.3 °C). Relative to simulations without ozone changes, there was an additional warming of 0.2 °C from 100 hPa to the top of the atmosphere, and 0.05 °C in most of the mid-latitude and tropical troposphere. Circulation changes (associated with the strength of wintertime westerlies) were also directly influenced by the inclusion of the ozone response. The exact pattern of ozone changes and temperature response will however be sensitive to uncertainties in the spectral variations in irradiance discussed above. Ideally, a new parameterisation could be made for each substantially different spectral estimate.

3 Discussion

Given the variation in plausible reconstructions of the forcings, input data and techniques used, it is clear that picking a single “best” set is fraught with difficulty. Even though it would be easiest for modelling groups to only use one set of reconstructions, the very real uncertainties associated with that choice would not be apparent in the range of simulations made available for analysis.

Given as well the undoubted public interest in the solar component of post-LIA climate change, and the perhaps disproportionate attention given to Medieval climate changes, picking any one reconstruction – each of which has different levels of medieval-to-modern and post-LIA change – might be seen as attempting to bias the results of the models.

We underline that these reconstructions are designed for a very specific purpose related to the PMIP3 simulations. They should not be used for sub-multi-decadal correlations to proxy data (since the high frequency variability is synthetic prior to the merge with WLS and very likely out of phase with the real quasi-decadal solar cycle). Neither should they be taken as an endorsement of the WLS, VSK or SBF estimates of the background changes at the Maunder Minimum. This calibration is still very much a focus of current research. Instead, we hope that the range of reconstructions given is wide enough so that the structural uncertainty in forcing can be appropriately taken into account in any climate change attribution studies.

There are undoubtedly further variations that could be assessed. For instance, use of the Krivova et al. (2010) spectral changes or any new reconstruction derived from the Harder et al. (2009) spectral changes might be warranted, particularly in simulations with interactive ozone. Furthermore, other TSI reconstructions are also being developed (Shapiro et al., 2010) which suggest a larger change in the Maunder Minimum, but which were not available for use at time of writing. We hope to be able to provide updates to these forcings over time.

It is worth briefly commenting on the structural implications of the various choices being made available. It is relatively straightforward to calculate the envelope of adjusted top-of-the-atmosphere (TOA) radiative forcing for the various solar TSI changes (dividing by 4 and multiplying by the co-albedo). Forcings from greenhouse gas changes can be derived using formulas from Houghton et al. (2001) (Table 6.2) and efficacies from Hansen et al. (2005) (in order to account for the slight variations in physical effects of each change and some indirect effects such as the change in stratospheric water vapour as a function of changes in methane oxidation). We include an estimate for the radiative forcing associated with land use/land cover for surface albedo changes (Pongratz et al., 2009). This may be model dependent (Pitman et al., 2009) and does not include the implied changes in CO_2 (which are implicit in the greenhouse gas records), or the effects of evapotranspiration changes (Davin et al., 2007; Pongratz et al., 2010). Changes in the global mean forcing associated with orbital changes are small as is the net forcing due to ozone-related changes (Shindell et al., 2006). The AOD time series for the volcanic reconstructions can be used to estimate the corresponding radiative forcing (in units of Wm^{-2}) by multiplying it by -20 (Wigley et al., 2005) (though other authors suggest a factor of -25, Sato et al., 1993), however this does not include a dependency on the r_e variations, which can make a substantial difference for the large eruptions.

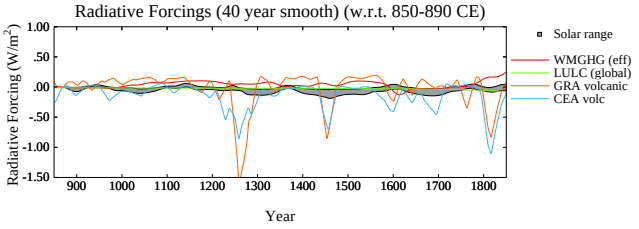

Fig. 9. Radiative forcing from well-mixed greenhouse gases (using the IPCC formulas and efficacy from Hansen et al., 2005), LULC-related albedo change (Pongratz et al., 2009), a smoothed envelope of solar forcing, and the two smoothed volcanic reconstructions. Smoothing is with a 40-year triangular filter.

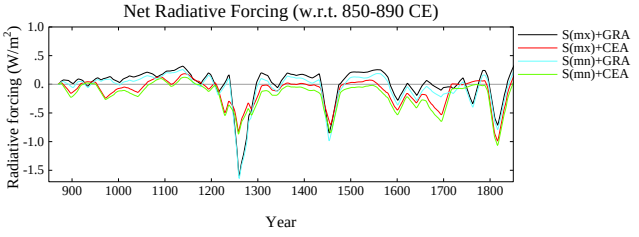

Fig. 10. The net radiative forcing encompassing variation from the solar envelope and the two volcanic reconstructions and smoothing as in Fig. 9. The zero-line is with reference to the earliest 40 year period.

Figure 9 shows each individual component (smoothed for clarity) while Fig. 10 shows the sum of all these effects to make a preliminary estimate of the global mean net effective TOA radiative forcing over time. Depending on the implementation of forcings and the model itself, the net forcing in any specific model simulation might be different, but this is a reasonable first order estimate of the likely impact on any model (c.f. Jansen et al., 2007, Fig. 6.13). Note that while the annual time series might be of use for intermediate complexity models (see Supplement), for GCMs we strongly suggest implementing the physical forcing as realistically as possible and calculating the resulting radiative forcing according to CMIP5 protocols.

The most obvious feature is the difference that the volcanic reconstructions make on even centennial variations of the forcing. Given the very long term impacts of large eruptions (Gleckler et al., 2006), this difference is likely to be important in modelled responses in the 13th/14th centuries and in the Maunder Minimum period. Comparatively, the choice of solar reconstruction may not be as obviously important, although they have more persistent effects over time. Compared to the forcing histories that have been used previously (Jansen et al., 2007), the volcanic reconstructions span a similar range in radiative forcing and eruption frequency, while the solar forcings are slightly reduced in

magnitude as discussed above. Greenhouse gas and orbital forcings are similar to that used previously. The new forcings presented here (land use, solar-ozone feedbacks) have only rarely or never been used before in simulations of this nature.

We anticipate that the global and hemispheric mean temperature changes in the model simulations will closely follow the smoothed forcing fields, though with amplitudes and lags that will vary depending on rates of ocean heat uptake and overall sensitivity. However, we also expect that the regional impact of various forcings will depend on the implementation of the forcing fields (whether the stratospheric aerosols are included as an absorbing and reflecting layer in the lower stratosphere, or imposed as a TOA radiative perturbation for instance), and the sensitivity of the model. While there is a higher amount of internal variability at the regional scale, long simulations and greater numbers of ensemble members will also be available for the analyses. Thus it is likely that the regional climate change fingerprints driven by the various forcings will be of most utility in assessing model skill (Mann et al., 2009; Schmidt, 2010).

Supplementary material related to this article is available online at: http://www.geosci-model-dev.net/4/33/2011/ gmd-4-33-2011-supplement.zip.

Acknowledgements. Thanks to Jean-Yves Peterschmitt for curating the PMIP website and wiki, Judith Lean for discussions and free access to her results and Sam Heilbroner for help in data processing. All the reconstructions and the annual estimated radiative forcing are available in the Supplement or from https://pmip3.lsce.ipsl.fr/wiki/doku.php/pmip3:design:lm:final. Thanks to all of the groups who sent in data, some of it unpublished. PAGES and the PAGES/CLIVAR Intersection Panel deserve special mention for facilitating discussions and meetings.

Edited by: J. C. Hargreaves

References

Balmaceda, L., Krivova, N. A., and Solanki, S. K.: Reconstruction of solar irradiance using the Group sunspot number, Adv. Space Res., 40, 986–989, 2007.

Beer, J., Tobias, A., and Weiss, B.: An active sun throughout the Maunder Minimum, Sol. Phys., 181, 237–249, 1998.

Berger, A.: Long-term variations of daily insolation and quaternary climatic changes, J. Atmos. Sci., 35, 2362–2367, 1978.

Berggren, A.-M., Beer, J., Possnert, G., Aldahan, A., Kubik, P., Christl, M., Johnsen, S. J., Abreu, J., and Vinther, B. M.: A 600-year annual ^{10}Be record from the NGRIP ice core, Greenland, Geophys. Res. Lett., 36, L11801, doi:10.1029/2009GL038004, 2009.

Braconnot, P., Otto-Bliesner, B., Harrison, S., Joussaume, S., Peterchmitt, J.-Y., Abe-Ouchi, A., Crucifix, M., Driesschaert, E., Fichefet, Th., Hewitt, C. D., Kageyama, M., Kitoh, A., Laîné, A., Loutre, M.-F., Marti, O., Merkel, U., Ramstein, G., Valdes, P., Weber, S. L., Yu, Y., and Zhao, Y.: Results of PMIP2 coupled simulations of the Mid-Holocene and Last Glacial Maximum - Part 1: experiments and large-scale features, Clim. Past, 3, 261–277, doi:10.5194/cp-3-261-2007, 2007.

Bradley, R. S., Hughes, M. K., and Diaz, H. F.: Climate in medieval time, Science, 302, 404–405, 2003.

Clilverd, M. A., Clarke, E., Ulich, T., Linthe, J., and Rishbeth, H.: Reconstructing the long-term *aa* index, J. Geophys. Res., 110, A07205, doi:10.1029/2004JA010762, 2005.

Crowley, T. J., Zielinski, G., Vinther, B., Udisti, R., Kreutzs, K., Cole-Dai, J., and Castellano, E.: Volcanism and the Little Ice Age, PAGES Newslett., 16, 22–23, 2008.

Davin, E. L., de Noblet-Ducoudré, N., and Friedlingstein, P.: Impact of land cover change on surface climate: relevance of the radiative forcing concept, Geophys. Res. Lett., 34, L13702, doi:10.1029/2007GL029678, 2007.

Delaygue, G. and Bard, E.: An Antarctic view of Beryllium-10 and solar activity for the past millennium, Clim. Dynam., in press, doi:10.1007/s00382-010-0795-1, 2010.

Dewitte, S., Crommelynck, D., Mekaoui, S., and Joukoff, A.: Measurement and uncertainty of the long-term Total Solar Irradiance trend, Sol. Phys., 224, 209–216, 2004.

Dickinson, R. E.: Solar variability and the lower atmosphere, B. Am. Meteor. Soc., 56, 1240–1248, 1975.

Etheridge, D. M., Steele, L. P., Langenfelds, R. L., Francey, R. J., Barnola, J. M., and Morgan, V. I.: Natural and anthropogenic changes in atmospheric CO_2 over the last 1000 years from air in Antarctic ice and firn, J. Geophys. Res., 101, 4115–4128, 1996.

Etheridge, D. M., Steele, L. P., Francey, R. J., and Langenfelds, R. L.: Atmospheric methane between 1000 AD and present: Evidence of anthropogenic emissions and climatic variability, J. Geophys. Res., 103, 15979–15996, 1998.

Ferretti, D. F., Miller, J. B., White, J. W. C., Etheridge, D. M., Lassey, K. R., Lowe, D. C., MacFarling Meure, C. M., Dreier, M. F., Trudinger, C. M., and van Ommen, T. D.: Unexpected changes to the global methane budget over the last 2000 years, Science, 309, 1714–1717, 2005.

Field, C. V., Schmidt, G. A., and Shindell, D. T.: Interpreting ^{10}Be changes during the Maunder Minimum, J. Geophys. Res., 114, D02113, doi:10.1029/2008JD010578, 2009.

Floyd, L., Rottman, G., DeLand, M., and Pap, J.: 11 years of solar UV irradiance measurements from UARS, in: Solar variability as an input to the Earth's environment, International Solar Cycle Studies (ISCS) Symposium, 23–28 June 2003, Tatranská Lomnica, Slovak Republic, edited by: Wilson, A., vol. 535 of ESA SP, ESA Publications Division, 195–203, 2003.

Flückiger, J., Dällenbach, A., Blunier, T., Stauffer, B., Stocker, T. F., Raynaud, D., and Barnola, J.-M.: Variations in atmospheric N_2O concentration during abrupt climatic changes, Science, 285, 227–230, 1999.

Flückiger, J., Monnin, E., Stauffer, B., Schwander, J., Stocker, T. F., Chappellaz, J., Raynaud, D., and Barnola, J.-M.: High resolution Holocene N_2O ice core record and its relationship with CH_4 and CO_2, Global Biogeochem. Cy., 16, 1010, doi:10.1029/2001GB001417, 2002.

Forster, P., Ramaswamy, V., Artaxo, P., Bernstein, T., Betts, R., Fahey, D. W., Haywood, J., Lean, J., Lowe, D. C., Myhre, G., Nganga, J., Prinn, R., Raga, G., Schultz, M., and Dorland, R. V.:

Changes in Atmospheric Constituents and in Radiative Forcing, in: Climate Change 2007: The Physical Science Basis, Contribution of Working Group I to the Fourth Assessment Report of the Intergovernmental Panel on Climate Change, edited by: Solomon, S., Qin, D., Manning, M., Chen, Z., Marquis, M., Averyt, K. B., Tignor, M., and Miller, H. L., Cambridge University Press, Cambridge, UK and New York, NY, USA, 2007.

Foukal, P., Fröhlich, C., Spruit, H., and Wigley, T. M. L.: Variations in solar luminosity and their effect on the Earth's climate, Nature, 443, 161–166, 2006.

Fröhlich, C.: Solar Irradiance variability since 1978, Revision of the PMOD composite during solar cycle 21, Space Sci. Rev., 125, 53–65, 2006.

Fröhlich, C.: Evidence of a long-term trend in total solar irradiance, Astron. Astrophys., 501, L27–L30, doi:10.1051/0004-6361/200912318, 2009.

Fröhlich, C. and Lean, J.: The Sun's total irradiance: Cycles and trends in the past two decades and associated climate change uncertainties, Geophys. Res. Lett., 25, 4377–4380, 1998.

Gao, C. C., Robock, A., and Ammann, C.: Volcanic forcing of climate over the past 1500 years: an improved ice core-based index for climate models, J. Geophys. Res., 113, D23111, doi:10.1029/2008JD010239, 2008.

Gerber, S., Joos, F., Bruegger, P. P., Stocker, T. F., Mann, M. E., and Sitch, S.: Constraining temperature variations over the last millennium by comparing simulated and observed atmospheric CO_2, Clim. Dynam., 20, 281–299, 2003.

Gleckler, P. J., AchutaRao, K., Gregory, J. M., Santer, B. D., Taylor, K. E., and Wigley, T. M. L.: Krakatoa lives: The effect of volcanic eruptions on ocean heat content and thermal expansion, Geophys. Res. Lett., 33, L17702, doi:10.1029/2006GL026771, 2006.

Gray, L. J., Beer, J., Geller, M., Haigh, J. D., Lockwood, M., Matthes, K., Cubasch, U., Fleitmann, D., Harrison, G., Hood, L., Luterbacher, J., Meehl, G. A., Shindell, D., van Geel, B., and White, W.: Solar influences on climate, Rev. Geophys., 48, RG4001, doi:10.1029/2009RG000282, 2010.

Hansen, J. and Sato, M.: Greenhouse gas growth rates, P. Natl. Acad. Sci. USA, 101, 16109–16114, 2004.

Hansen, J. E., Sato, M., Ruedy, R., Nazarenko, L., Lacis, A., Schmidt, G. A., Russell, G., Aleinov, I., Bauer, M., Bauer, S., Bell, N., Cairns, B., Canuto, V., Chandler, M., Cheng, Y., Genio, A. D., Faluvegi, G., Fleming, E., Friend, A., Hall, T., Jackman, C., Kelley, M., Kiang, N. Y., Koch, D., Lean, J., Lerner, J., Lo, K., Menon, S., Miller, R. L., Minnis, P., Novakov, T., Oinas, V., Perlwitz, J., Perlwitz, J., Rind, D., Romanou, A., Shindell, D., Stone, P., Sun, S., Tausnev, N., Thresher, D., Wielicki, B., Wong, T., Yao, M., and Zhang, S.: Efficacy of Climate Forcings, J. Geophys. Res., 110, D18104, doi:10.1029/2005JD005776, 2005.

Harder, J. W., Fontenla, J. M., Pilewskie, P., Richard, E. C., and Woods, T. N.: Trends in solar spectral irradiance variability in the visible and infrared, Geophys. Res. Lett., 36, L07801, doi:10.1029/2008GL036797, 2009.

Hegerl, G. C., Zwiers, F. W., Braconnot, P., Gillett, N. P., Luo, Y., Orsini, J. A. M., Nicholls, N., Penner, J. E., and Stott, P. A.: Understanding and Attributing Climate Change, in: Climate Change 2007: The Physical Science Basis, Contribution of Working Group I to the Fourth Assessment Report of the Intergovernmental Panel on Climate Change, edited by: Solomon, S., Qin, D., Manning, M., Chen, Z., Marquis, M., Averyt, K. B., Tignor, M., and Miller, H. L., Cambridge University Press, Cambridge, UK and New York, NY, USA, 2007.

Heikkilä, U., Beer, J., and Feichter, J.: Modeling cosmogenic radionuclides ^{10}Be and ^{7}Be during the Maunder Minimum using the ECHAM5-HAM General Circulation Model, Atmos. Chem. Phys., 8, 2797–2809, doi:10.5194/acp-8-2797-2008, 2008.

Horiuchi, K., Uchida, T., Sakamoto, Y., Ohta, A., Matsuzaki, H., Shibata, Y., and Motoyama, H.: Ice core record of ^{10}Be over the past millennium from Dome Fuji, Antarctica: A new proxy record of past solar activity and a powerful tool for stratigraphic dating, Quat. Geochronol., 3, 253–261, 2008.

Houghton, J. T., Ding, Y., Griggs, D. J., Nouger, M., van der Linden, P. J., Dai, X., Maskell, K., and Johnson, C. A.: Climate Change 2001: The scientific basis, Cambridge Univ. Press, New York, 2001.

Hoyt, D. V. and Schatten, K. H.: Group sunspot numbers: A new solar activity reconstruction, Sol. Phys., 181, 491–512, 1998.

Hurtt, G. C., Chini, L. P., Frolking, S., Betts, R., Feedema, J., Fischer, G., Goldewijk, K. K., Hibbard, K., Janetos, A., Jones, C., Kindermann, G., Kinoshita, T., Riahi, K., Shevliakova, E., Smith, S., Stehfest, E., Thomson, A., Thorton, P., van Vuuren, D., and Wang, Y.: Harmonization of global land-use scenarios for the period 1500–2100 for IPCC-AR5, Integr. Land Ecosys.-Atmos. Process. Stud. (iLEAPS) Newslett., 7, 6–8, 2009.

Jansen, E., Overpeck, J., Briffa, K. R., Duplessy, J.-C., Joos, F., Masson-Delmotte, V., Olago, D., Otto-Bliesner, B., Peltier, W. R., Rahmstorf, S., Ramesh, R., Raynaud, D., Rind, D., Solomina, O., Villalba, R., and Zhang, D.: Palaeoclimate, in: Climate Change 2007: The Physical Science Basis, Contribution of Working Group I to the Fourth Assessment Report of the Intergovernmental Panel on Climate Change, edited by: Solomon, S., Qin, D., Manning, M., Chen, Z., Marquis, M., Averyt, K. B., Tignor, M., and Miller, H. L., Cambridge University Press, Cambridge, UK and New York, NY, USA, 2007.

Joos, F. and Spahni, R.: Rates of change in natural and anthropogenic radiative forcing over the past 20 000 years, P. Natl. Acad. Sci. USA, 105, 1425–1430, 2008.

Joussaume, S. and Taylor, K. E.: Status of the Paleoclimate Modeling Intercomparison Project (PMIP), in: Proceedings of the first international AMIP scientific conference, WCRP Report, 425–430, 1995.

Klein Goldewijk, K. and van Drecht, G.: HYDE3: Current and historical population and land cover, in: Integrated modelling of global environmental change, An overview of IMAGE 2.4, edited by: Bouwman, A. F., Kram, T., and Goldewijk, K. K., Netherlands Environmental Assessment Agency (MNP), Bilthoven, The Netherlands, 2006.

Kopp, G., Lawrence, G., and Rottman, G.: The Total Irradiance Monitor (TIM): Science results, Sol. Phys., 230, 129–139, doi:10.1007/s11207-005-7433-9, 2005.

Krivova, N. A., Solanki, S. K., Fligge, M., and Unruh, Y. C.: Reconstruction of solar irradiance variations in cycle 23: is solar surface magnetism the cause?, Astron. Astrophys., 399, L1–L4, 2003.

Krivova, N. A., Balmaceda, L., and Solanki, S. K.: Reconstruction of solar total irradiance since 1700 from the surface magnetic flux, Astron. Astrophys., 467, 335–346, 2007.

Krivova, N. A., Solanki, S. K., and Wenzler, T.: ACRIM – gap and total solar irradiance revisited: Is there a secular trend between 1986 and 1996?, Geophys. Res. Lett., 36, L20101, doi:10.1029/2009GL040707, 2009.

Krivova, N. A., Vieira, L. E. A. and Solanki, S. K.: Reconstruction of solar spectral irradiance since the Maunder Minimum, J. Geophys. Res., in press, 115, A12112, doi:10.1029/2010JA015431, 2010.

Laskar, J., Robutel, P., Joutel, F., Gastineau, M., Correia, A. C. M., and Levrard, B.: A long-term numerical solution for the insolation quantities of the Earth, Astron. Astroph., 428, 261–285, doi:10.1051/0004-6361:20041335, 2004.

Lean, J.: Evolution of the sun's spectral irradiance since the Maunder Minimum, Geophys. Res. Lett., 27, 2425–2428, 2000.

Lean, J.: Calculations of Solar Irradiance, http://www.geo.fu-berlin.de/en/met/ag/strat/forschung/SOLARIS/Input_data/Calculations_of_Solar_Irradiance.pdf, last access: 20 September 2010, 2009.

Lean, J., Beer, J., and Bradley, R.: Reconstruction of solar irradiance since 1610: Implications for climate change, Geophys. Res. Lett., 22, 3195–3198, 1995.

Lockwood, M., Stamper, R., and Wild, M. N.: A doubling of the Sun's coronal magnetic field during the past 100 years, Nature, 399, 437–439, 1999.

MacFarling Meure, C., Etheridge, D., Trudinger, C., Steele, P., Langenfelds, R., van Ommen, T., Smith, A., and Elkins, J.: Law Dome CO_2, CH_4 and N_2O ice core records extended to 2000 years BP, Geophys. Res. Lett., 33, L14810, doi:10.1029/2006GL026152, 2006.

Machida, T., Nakazawa, T., Fujii, Y., Aoki, S., and Watanabe, O.: Increase in the atmospheric nitrous oxide concentration during the last 250 years, Geophys. Res. Lett., 22, 2921–2924, 1995.

Mann, M. E., Zhang, Z., Rutherford, S., Bradley, R. S., Hughes, M. K., Shindell, D., Ammann, C., Faluvegi, G., and Ni, F.: Global signatures and dynamical origins of the Little Ice Age and Medieval Climate Anomaly, Science, 326, 1256–1260, 2009.

McCracken, K. G. and Beer, J.: Long-term changes in the cosmic ray intensity at Earth, J. Geophys. Res., 112, A10101, doi:10.1029/2006JA012117, 2007.

McCracken, K. G. and Heikkila, B.: The cosmic ray intensity between 1933 and 1965, in: 28th Cosmic Ray Conference, Tsukuba, Japan, vol. 7, 4117–4120, 2003.

Mekaoui, S., Dewitte, S., Conscience, C., and Chevalier, A.: Total solar irradiance absolute level from DIARAD/SOVIM on the International Space Station, Adv. Space Res., 45, 1393–1406, doi:10.1016/j.asr.2010.02.014, 2010.

Muscheler, R., Beer, J., Wagner, G., Laj, C., Kissel, C., Raisbeck, G. M., Yiou, F., and Kubik, P. W.: Changes in the carbon cycle during the last deglaciation as indicated by the comparison of ^{10}Be and ^{14}C records, Earth Planet. Sc. Lett., 219, 325–340, doi:10.1016/S0012-821X(03)00722-2, 2004.

Muscheler, R., Joos, F., Beer, J., Müller, S., Vonmoos, M., and Snowball, I.: Solar activity during the last 1000 yr inferred from radionuclide records, Quaternary Sci. Rev., 26, 82–97, doi:10.1016/j.quascirev.2006.07.012, 2007.

Ney, E. P.: Cosmic radiation and weather, Nature, 183, 451–452, 1959.

Osborn, T. J. and Briffa, K. R.: The spatial extent of 20th-century warmth in the context of the past 1200 years, Science, 311, 841, doi:10.1126/science.1120514, 2006.

Otto-Bliesner, B. L., Joussaume, S., Braconnot, P., Harrison, S. P., and Abe-Ouchi, A.: Modeling and data syntheses of past climates, EOS T. Am. Geophys. Un., doi:10.1029/2009EO110013, 2009.

Pitman, A. J., de Noblet-Ducoudré, N., Cruz, F. T., Davin, E. L., Bonan, G. B., Brovkin, V., Claussen, M., Delire, C., Ganzeveld, L., Gayler, V., van den Hurk, B. J. J. M., Lawrence, P. J., van der Molen, M. K., Müller, C., Reick, C. H., Seneviratne, S. I., Strengers, B. J., and Voldoire, A.: Uncertainties in climate responses to past land cover change: first results from the LUCID intercomparison study, Geophys. Res. Lett, 36, L14814, doi:10.1029/2009GL039076, 2009.

Pongratz, J., Reick, C. H., Raddatz, T., and Claussen, M.: A reconstruction of global agricultural areas and land cover for the Last Millennium, Global Biogeochem. Cy., 22, GB3018, doi:10.1029/2007GB003153, 2008.

Pongratz, J., Raddatz, T., Reick, C. H., Esch, M., and Claussen, M.: Radiative forcing from anthropogenic land cover change since AD 800, Geophys. Res. Lett., 36, L02709, doi:10.1029/2008GL036394, 2009.

Pongratz, J., Reick, C. H., Raddatz, T., and Claussen, M.: Biogeophysical versus biogeochemical climate response to historical anthropogenic land cover change, Geophys. Res. Lett., 37, L08702, doi:10.1029/2010GL043010, 2010.

Raisbeck, G. M., Yiou, F., Jouzel, J., and Petit, J. R.: ^{10}Be and δ^2H in polar ice cores as a probe of the solar variability's influence on climate, Philos. T. Roy. Soc. Lond. A, 330, 463–470, doi:10.1098/rsta.1990.0027, 1990.

Ramankutty, N. and Foley, J. A.: Estimating historical changes in global land cover: Croplands from 1700 to 1992, Global Biogeochem. Cy., 1, 997–1027, 1999.

Reimer, P. J., Baillie, M. G. L., Bard, E., Bayliss, A., Beck, J. W., Blackwell, P. G., Ramsey, C. B., Buck, C. E., Burr, G. S., Edwards, R. L., Friedrich, M., Grootes, P. M., Guilderson, T. P., Hajdas, I., Heaton, T. J., Hogg, A. G., Hughen, K. A., Kaiser, K. F., Kromer, B., McCormac, F. G., Manning, S. W., Reimer, R. W., Richards, D. A., Southon, J. R., Talamo, S., Turney, C. S. M., van der Plicht, J., and Weyhenmeyer, C. E.: IntCal09 and Marine09 radiocarbon age calibration curves, 0–50 000 years cal BP, Radiocarbon, 51, 1111–1150, 2009.

Rouillard, A. P., Lockwood, M., and Finch, I.: Centennial changes in the solar wind speed and in the open solar flux, J. Geophys. Res., 112, A05103, doi:10.1029/2006JA012130, 2007.

Sato, M., Hansen, J. E., McCormick, M. P., and Pollack, J. B.: Stratospheric aerosol optical depths, 1850–1990, J. Geophys. Res., 98, 22987–22994, 1993.

Schmidt, G. A.: Enhancing the relevance of palaeoclimate model/data comparisons for assessments of future climate change, J. Quaternary Sci., 25, 79–87, doi:10.1002/jqs.1314, 2010.

Shapiro, A., Schmutz, W., Thuillier, G., Schoell, M., Haberreiter, M., and Rozanov, E.: Modeling of the Current TSI and SSI and its Reconstruction to the Past, Tech. Rep., 38th COSPAR Scientific Assembly, 2010.

Shindell, D. T., Faluvegi, G., Miller, R. L., Schmidt, G. A., Hansen, J. E., and Sun, S.: Solar and anthropogenic forcing of tropical hydrology, Geophys. Res. Lett., 33, L24706, doi: 10.1029/2006GL027468, 2006.

Soukharev, B. E. and Hood, L. L.: Solar cycle variation of stratospheric ozone: Multiple regression analysis of longterm satellite data sets and comparisons with models, J. Geophys. Res., 111, D20314, doi:10.1029/2006JD007107, 2006.

Steinhilber, F., Beer, J., and Fröhlich, C.: Total solar irradiance during the Holocene, Geophys. Res. Lett., 36, L19704, doi: 10.1029/2009GL040142, 2009.

Stothers, R. B.: The Great Tambora Eruption in 1815 and its aftermath, Science, 224, 1191–1198, doi:10.1126/science.224. 4654.1191, 1984.

Svalgaard, L., Cliver, E. W., and Sager, P. L.: IHV: A new long-term geomagnetic index, Adv. Space. Res., 34, 436–439, 2004.

Tanaka, H., Castelli, J. P., Covington, A. E., Krüger, A., Landecker, T. L., and Tlamicha, A.: Absolute calibration of solar radio flux density in the microwave region, Sol. Phys., 29, 243–262, doi:10.1007/BF00153452, 1973.

Taylor, K. E., Stouffer, R. J., and Meehl, G. A.: A Summary of the CMIP5 Experiment Design, http://cmip-pcmdi.llnl.gov/cmip5/docs/Taylor_CMIP5_design.pdf, last access: 20 September 2010, 2009.

Timmreck, C., Lorenz, S. J., Crowley, T. J., Kinne, S., Raddatz, T. J., Thomas, M. A., and Jungclaus, J. H.: Limited temperature response to the very large AD 1258 volcanic eruption, Geophys. Res. Lett., 36, L21708, doi:10.1029/2009GL040083, 2009.

Usoskin, I. G., Mursula, K., Solanki, S. K., Schüssler, M., and Kovaltsov, G. A.: Physical reconstruction of cosmic ray intensity since 1610, J. Geophys. Res., 107, 1374, doi:10.1029/2002JA009343, 2002.

Usoskin, I. G., Horiuchi, K., Solanki, S., Kovaltsov, G. A., and Bard, E.: On the common solar signal in different cosmogenic isotope data sets, J. Geophys. Res., 114, A03112, doi:10.1029/2008JA013888, 2009.

Vieira, L. E. A., Solanki, S. K., Krivova, N. A., and Usoskin, I.: Evolution of the solar irradiance on time scales of years to millennia, Astron. Astrophys., submitted, 2010.

Viereck, R. A., Floyd, L. E., Crane, P. C., Woods, T. N., Knapp, B. G., Rottman, G., Weber, M., and Puga, L. C.: A composite Mg II index spanning from 1978 to 2003, Adv. Space Res., 2, S10005, doi:10.1029/2004SW000084, 2004.

Vonmoos, M., Beer, J., and Muscheler, R.: Large variations in Holocene solar activity: Constraints from ^{10}Be in the Greenland Ice Core Project ice core, J. Geophys. Res., 111, A10105, doi: 10.1029/2005JA011500, 2006.

Wang, Y.-M., Lean, J. L., and Sheeley Jr., N. R.: Modeling the Sun's Magnetic Field and Irradiance since 1713, Astrophys. J., 625, 522–538, doi:10.1086/429689, 2005.

Wenzler, T., Solanki, S. K., Krivova, N. A., and Fluri, D. M.: Comparison between KPVT/SPM and SoHO/MDI magnetograms with an application to solar irradiance reconstructions, Astron. Astrophys., 427, 1031–1043, 2004.

Wenzler, T., Solanki, S. K., Krivova, N. A., and Fröhlich, C.: Reconstruction of solar irradiance variations in cycles 21–23 based on surface magnetic fields, Astron. Astrophys., 460, 583–595, 2006.

Wigley, T. M. L., Ammann, C. M., Santer, B. D., and Raper, S. C. B.: Effect of climate sensitivity on the response to volcanic forcing, J. Geophys. Res., 110, D09107, doi:10.1029/2004JD005557, 2005.

Willson, R. C. and Mordvinov, A. V.: Secular total solar irradiance trend during solar cycles 21–23, Geophys. Res. Lett., 30, 1199, doi:10.1029/2002GL016038, 2003.

Yiou, F., Raisbeck, G. M., Baumgartner, S., Beer, J., Hammer, C., Johnsen, S., Jouzel, J., Kubik, P. W., Lestringuez, J., Stiévenard, M., Suter, M., and Yiou, P.: Beryllium 10 in the Greenland Ice Core Project ice core at Summit, Greenland, J. Geophys. Res., 102, 26783–26794, 1997.